JOURNAL OF MATERIALS SCIENCE 29 (1994) 2078–2082

Influence of surface oxidation on thermal shock resistance and flexural strength of SiC/Al_2O_3 composites

CHIN-CHEN CHIU
Van Zion Company, Taoyuan, Taiwan, Republic of China

It is known that SiC whisker/Al_2O_3 matrix composites can oxidize in air at high temperature and then form oxidation layers on their surfaces. Oxidation treatment has been experimentally performed in air at 1450 °C for a pre-determined time. The results show that the surface layer is in a state of compressive residual stress. The oxidized specimens have better resistance to thermal shock damage than the non-oxidized specimens. However, the surface oxidation can degrade the room-temperature flexural strength.

1. Introduction

The SiC whisker reinforcement of alumina can improve the mechanical properties, such as toughness, [1, 2], erosive wear resistance [3], high-temperature flexural strength [4], creep resistance [5, 6], and thermal shock resistance [7]. As a result, SiC whisker/Al_2O_3 matrix composites are promising candidates in structural high-temperature applications. However, SiC/Al_2O_3 composites can oxidize in air at high temperature and produce aluminosilicate glass–mullite layers, accompanied by carbon monoxide-induced bubbles, on their surfaces [6, 8]. Thus, the effect of the surface oxidation on mechanical properties should be studied.

As a result of the change in composition and microstructure [6, 8], the surface layer behaves as an extra ceramic coating on the specimens. Consequently, the integrated mechanical properties of the specimens could obviously be influenced. For example, the surface compressive residual stress, caused by the thermal expansion mismatch between the surface layer and the unreacted core, could strengthen the specimens. The layer may change surface heat-transfer conditions and thus affect the resistance to thermal shock damage [9]. The oxidation-induced bubbles may degrade the fracture strength, because the fracture strength of brittle materials is sensitive to the variation of surface flaw size.

In the present paper, hot isostatic pressing SiC/Al_2O_3 composite specimens were exposed to air at 1450 °C for the desired time. The residual stress in the surface oxidation layer was measured using a strain gauge technique [10, 11]. The resistance to thermal shock damage was evaluated by means of thermal quench testing and elastic modulus measurement [12–14]. Flexural strength was measured using three-point bending.

2. Experimental procedure

2.1. Materials and oxidation treatment

Hot isostatic pressing SiC whisker/Al_2O_3 composites (provided by Andre Ezis, Cercom Incorporated, Vista, CA) were used in this study. The composites contained 27% by weight of SiC whisker and had a density of 3.73 g cm^{-3}. Using a diamond saw, as-received composite tiles were cut into specimens 3 cm × 0.2 cm × 0.2 cm, 7.6 cm × 0.7 cm × 0.2 cm, and 7.6 cm × 0.7 cm × 0.1 cm in size. Specimen surfaces were polished using diamond paste (1 μm).

Oxidation reaction treatment was carried out in air in an $MoSi_2$ heating element furnace. Specimens were supported at two ends using alumina rods to ensure the air exposure of all surfaces. The furnace temperature was increased to 1450 °C at a heating rate of about 40 °C min^{-1} and was maintained for the desired time. Specimens were then furnace cooled at a rate of about 30 °C min^{-1}. The maximum time of the oxidation treatment was 85 h.

2.2. Surface residual stress

Using a strain gauge technique [10, 11], the residual stress in the surface oxidation layer was measured on the specimens (7.6 cm × 0.7 cm × 0.2 cm and 7.6 cm × 0.7 cm × 0.1 cm) oxidized at 1450 °C for 85 h. Five surfaces of a specimen, except one 7.6 cm × 0.7 cm surface, were first polished to remove oxidation products. A curvature then developed in the polished specimen. A strain gauge (EA-06-125BZ-350, Measurements Group Inc., Raleigh, NC) was attached to the polished 7.6 cm × 0.7 cm surface, parallel to specimen's long axis (see Fig. 1). When the oxidation products on the unpolished 7.6 cm × 0.7 cm surface were finally removed, the strain gauge detected a strain ε_{s*}. The strain was associated with the curvature. The residual stress in the surface layer, σ^*, was calculated from ε_{s*} using following equation [11]

$$\sigma^* = -\frac{E_s\varepsilon_{s*}R(E_sR^3 + E_c)}{2E_sR^3 + 3E_sR^2 - E_c} \quad (1a)$$

where

$$R = \frac{l_s}{l_c} \quad (1b)$$

0022–2461 © *1994 Chapman & Hall*

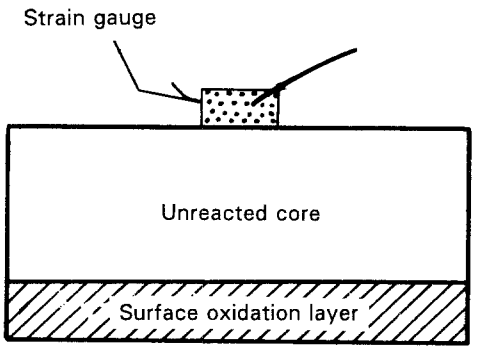

Figure 1 Schematic drawing of the strain gauge apparatus for measuring surface strain.

The subscripts, c and s, refer to properties of the surface oxidation layer and the unreacted core, respectively. E and l are the elastic modulus and the thickness, respectively. The oxidation layer thickness was measured from the fracture surface of the oxidized specimen using an optical microscope. Previous work [8] showed that E_c and E_s were 159 and 403 GPa, respectively.

2.3. Thermal shock testing

The as-polished specimens (7.6 cm × 0.7 cm × 0.2 cm) and the specimens oxidized at 1450 °C for 85 h were heated from room temperature in an electrical furnace. When the furnace temperature was stable for at least half an hour, the specimens were quenched into a distilled water bath of 20 °C. The shock-induced damage was evaluated by means of the dynamic elastic modulus measurement [12–14]. The measurement technique was described elsewhere [15]. To observe crack healing, the shocked specimens were oxidized in a furnace at 1450 °C for 2 h. The specimens were then examined using an optical microscope and a scanning electron microscope (SEM) with an energy dispersive X-ray analysis unit.

Commercial alumina substrate specimens were also tested to compare with SiC/Al_2O_3 composites. Specimens 10.0 cm × 0.9 cm × 0.2 cm were cut from as-received substrates (supplied by Frank Fandetti, Hoechst CeramTec North America Incorporated, Mansfield, MA) and then annealed at 1100 °C for 10 h. The annealed alumina specimens were thermally shocked as described as above.

2.4. Flexural strength

Room-temperature flexural strength was tested on 3 cm × 0.2 cm × 0.2 cm specimens in three-point bending at a crosshead speed of 0.1 cm min^{-1} with a span of 2.2 cm. The flexural strength data were analysed on the basis of two parameter Weibull distribution function [16], namely,

$$F(y) = 1 - \exp[-(y/\beta)^m] \quad (2)$$

where $F(y)$ is cumulative density function. β and m are a scale parameter and the Weibull modulus, respectively, which are calculated according to the maximum likelihood estimating function [17]. The expected value $E(y)$ and the variance $V(y)$ are [16]

$$E(y) = \beta\Gamma(1 + 1/m) \quad (3a)$$

$$V(y) = \beta^2[\Gamma(1 + 2/m) - \Gamma^2(1 + 1/m)] \quad (3b)$$

where Γ is the gamma function.

3. Results

When SiC whisker/Al_2O_3 composite specimens were exposed to air at 1450 °C, the SiC whisker was oxidized and then reacted with alumina to produce a reaction layer on the surface of the specimens. Fig. 2 is an optical micrograph of the fracture surface of an oxidized specimen, showing that the surface layer exhibits a darker colour than the unreacted core. Oxidation-induced bubbles appear near the surface layer/unreacted core interface, rather than the overall layer. Because the layer behaves as a ceramic coating, the thermal expansion mismatch between the surface layer and the unreacted core results in thermal residual stress. The curvature developed in an oxidized specimen, with five surface oxidation layers being polished off, is an index from which the residual stress can be determined. A strain-gauge technique reveals that all specimens exhibit convex curvature on the unpolished side. Thus, the surface oxidation layer is in compressive stress. Each point in Fig. 3 corresponds to one specimen. The solid curve is a regression curve, which is plotted according to the experimental data and the equation (B-5) given in [10]. The compressive residual stress increases with increase of R, the ratio of the unreacted core thickness to the surface layer thickness. The experimental result agrees with theoretical prediction [10, 11].

Thermal shock damage is typically evaluated via the fracture strength measurement. However, elastic modulus can also be a useful indicator of thermal shock damage, because the decrease in observed elastic modulus, ΔE, reflects the total accumulation of shock-induced cracks [12–14]. The moduli of unshocked specimens of monolithic alumina, as-polished composites, and oxidized composites are 303, 403 and

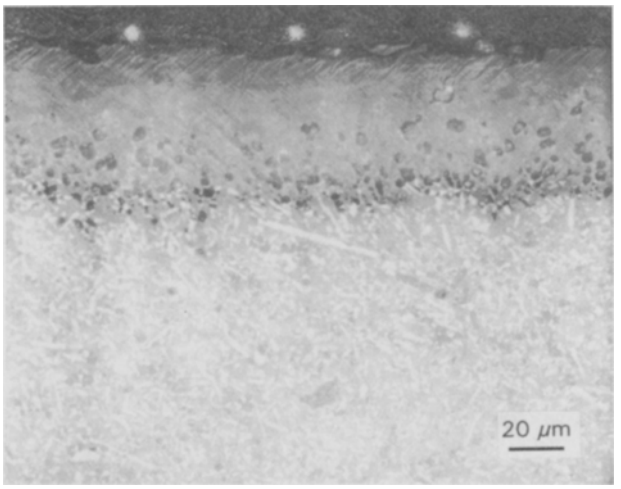

Figure 2 An optical micrograph of the fracture surface of the specimen oxidized at 1450 °C for 37 h.

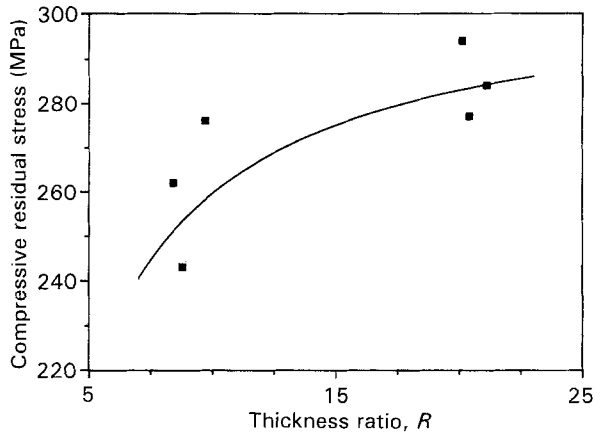

Figure 3 A plot of surface residual stress versus the ratio of unreacted core thickness to surface layer thickness. The specimens were oxidized at 1450 °C for 85 h and had surface layers of about 78 μm.

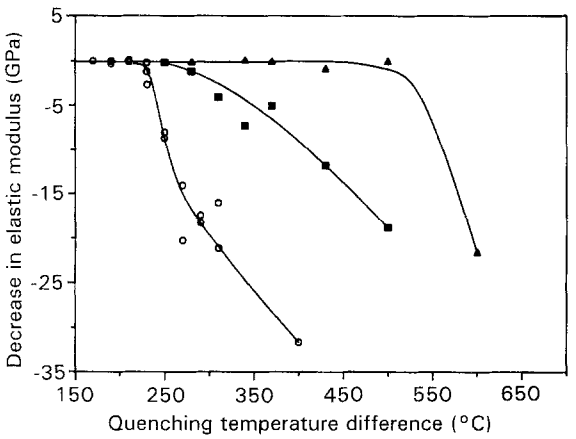

Figure 4 Decrease in elastic modulus as a function of quenching temperature difference. Each point corresponds to one specimen. (○) Monolithic alumina, (■) as-polished SiC/Al_2O_3 specimens, (△) composite specimens with 85 h oxidation treatment.

300 GPa, respectively. A plot of ΔE versus quenching temperature difference, ΔT, shows that monolithic alumina, as-polished composites, and oxidized composites are not subjected to thermal shock damage until $\Delta T \approx 250$, 300 and 500 °C, respectively (Fig. 4). The degree of shock damage gradually deteriorates with further increase in ΔT. Thus, inspection of Fig. 4 indicates that the SiC/Al_2O_3 composites have better thermal shock resistance in comparison with the monolithic alumina, which agrees with the result given by Tiegs and Becher [7]. In addition, surface oxidation reaction enhances the thermal shock resistance of SiC/Al_2O_3 composites. The improvement in shock resistance is apparently associated with the surface oxidation layer, which will be further analysed in Section 4.

To observe the crack-healing phenomenon, a specimen with shock-induced cracks (Fig. 5a) was exposed to air at 1450 °C for 2 h. Because the surface oxidation layer obscured the underlying microstructural features, the surface layer was polished off. Fig. 5b shows a scanning electron micrograph of the polished specimen, indicating that the shock-induced cracks heal up and oxidation-induced bubbles arise on both sides of the crack trace. Energy dispersive X-ray analysis indicates that silicon and aluminium element concentration gradients exist from the crack trace toward the specimen's interior (see Fig. 5b and Fig. 6). The element concentration profiles are attributed to the oxidation of SiC whisker and the reaction SiC–oxygen–alumina. (The oxidation kinetics and mechanism was presented in a previous paper [8]). Thus, it is evident that surface oxidation reaction can enhance crack healing for those cracks which are open outwards towards the free surface. A crack groove provides a short cut for oxygen diffusion. Oxidation reaction extends from the crack surface towards the specimen's interior. Reaction products then fill in and blunt the crack groove.

Fig. 7 illustrates flexural strength distributions of the SiC/Al_2O_3 composite specimens under various surface treatments, in which each data point corresponds to one specimen. The strength data are analysed according to Weibull statistics. The cumulative

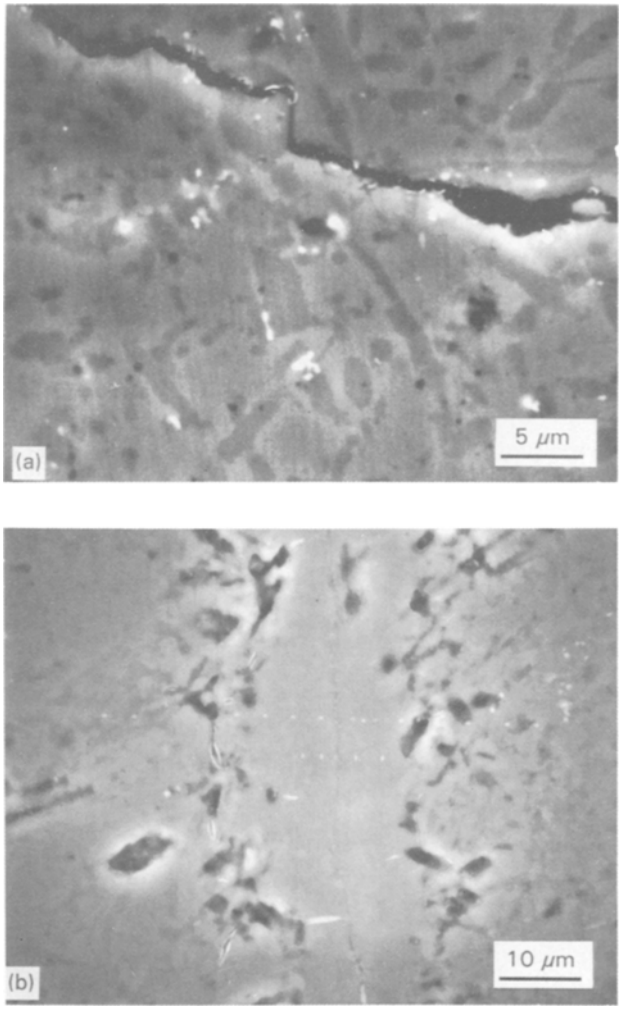

Figure 5 (a) Scanning electron micrograph of the specimen with shock-induced cracks. (b) Crack healing after the specimen was oxidized at 1450 °C for 2 h.

density distribution curves are plotted on the basis of the Weibull parameters listed in Table I. A comparison indicates that the strength distributions shift to lower strength after 2 and 85 h exposure to air. Oxidation treatment causes an increase of the variance $V(y)$. The composite specimens under three different surface

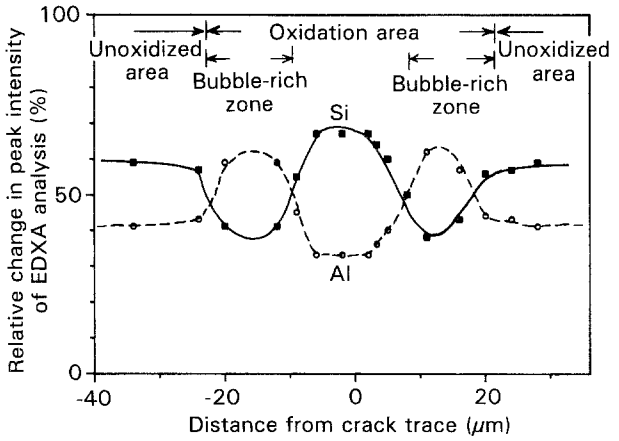

Figure 6 Element concentration profiles of a cracked specimen after exposure to air at 1450 °C for 2 h (see Fig. 5b). The profiles are plotted according to the ratio of the peak intensity of energy dispersive X-ray analysis [8]. Al% + Si% = 100%.

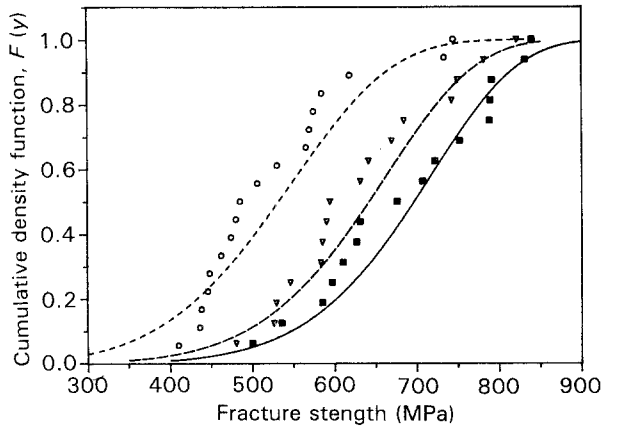

Figure 7 Fracture strength distributions of SiC/Al_2O_3 specimens after oxidation treatment. (■) As-polished specimens, (▽) specimens with 2 h oxidation treatment, (○) specimens with 85 h oxidation treatment.

treatments present somewhat different $E(y)$. The expected value, $E(y)$, of flexural strength of as-polished specimens is 687 MPa, while the specimens exposed at 1450 °C for 2 and 85 h correspond to 633 and 525 MPa, respectively. Therefore, analysis (the Mann–Whitney U test [18]) was carried out to determine whether or not the differences in $E(y)$ were statistically significant. The null hypothesis was that the oxidation treatment did not cause a change in $E(y)$. At a significance level of $\alpha = 0.05$, the analysis indicated that the oxidation treatment at 1450 °C for 2 h did not result in statistically significant change in $E(y)$. However, the oxidation treatment at 1450 °C for 85 h produced a decrease in $E(y)$. Thus, long periods of surface oxidation treatment tend to decrease flexural strength.

4. Discussion

Thermal quenching of hot specimens into a water bath causes transient thermal stresses, by which the specimens may encounter thermal shock damage. The critical quenching temperature difference for shock damage, ΔT_c, can be evaluated according to the heat-transfer conditions in which the maximum of the transient thermal stress at the specimen's surface is just equal to the fracture strength, σ_c. That is [19]

$$\sigma_c = \frac{\Delta T_c \alpha E F(B)}{1 - \nu} \tag{4a}$$

$$\frac{1}{F(B)} \approx 1.5 + \frac{3.25}{B} - 0.5 \exp\left(-\frac{16}{B}\right) \tag{4b}$$

$$B = \frac{ah}{k} \tag{4c}$$

where α, E, and ν are the thermal expansion coefficient, elastic modulus, and Poisson's ratio, respectively. B, a, h, and K are the Biot's modulus, characteristic length, surface heat-transfer coefficient, and thermal conductivity of specimen, respectively [19]. Fig. 4 illustrates that the specimens oxidized at 1450 °C for 85 h have an increasing resistance to thermal shock damage as compared with the non-oxidized specimens. The critical quenching temperature difference increases from $\Delta T_c \approx 300$ °C to $\Delta T_c \approx 500$ °C. However, Table I shows that the oxidation treatment decreases the flexural strength from 687 MPa to 525 MPa. Inspection of Equation 4a reveals that the increasing resistance to thermal shock damage is due to the decrease in $F(B)$, because α, E, ν, a, and k are material constants. Thus, it is concluded that the surface heat-transfer coefficient of oxidized specimens is smaller than that of non-oxidized specimens (see Equations 4b and 4c). The surface oxidation layer behaves as an extra coating on composite specimens and decreases the surface heat-transfer rate. In addition to the present work, Lewis also presented a study of the effect of surface treatment on the thermal shock behaviour [9]. He indicated that a chemically leached porous surface could decline the heat-transfer rate and improve the thermal shock resistance of glass–ceramic specimens [9].

TABLE I Weibull parameters for flexural strength data of the SiC/Al_2O_3 specimens under various surface treatments

Specimen	No. of specimens	Scale parameter (MPa)	Weibull modulus	Expected value (MPa)	Variance $(MPa)^2$	Maximum deviation[a] of K–S test
As-polished	16	731	7.8	687	10955	0.164
2 h oxidation	16	677	7.0	633	11282	0.170
85 h oxidation	18	569	5.5	525	12205	0.159

[a] This paper uses the Kolmogorov–Smirnov test (a goodness-of-fit test) to measure the discrepancy between the flexural strength data and the Weibull distribution function. At a significance level of $\alpha = 0.05$, a good fit requires that the maximum deviation does not exceed 0.3094 [18]. It is clear that the Weibull distribution function fits the strength data well.

The fracture strength of brittle materials is sensitive to surface flaw size so that surface oxidation treatment may obviously change the flexural strength. As indicated, the oxidation treatment of SiC/Al_2O_3 composite specimens can cause crack healing, surface compressive stress layers, and oxidation-induced bubbles. The cracking healing may blunt the crack tip and then strengthen the oxidized specimens. The surface compressive stress layer can increase the flexural strength, since the compressive stress must be overcome in addition to the original fracture strength in order to cause failure [20]. In contrast, the oxidation-induced bubbles tend to create new, large, surface flaws and weaken the specimens. In the oxidation treatment, these mechanisms may occur simultaneously and be in competition to control the overall strength behaviour. Table I shows that the flexural strength of composite specimens decreases from 687 MPa to 525 MPa after exposure to air at 1450 °C for 85 h. The strength degradation is attributed to the predominant effect of oxidation-induced bubbles.

The flexural strengths of as-polished specimens and the specimens oxidized at 1450 °C for 2 h correspond to $E(y) = 687$ and 633 MPa, respectively. Statistical analysis reveals that there is insufficient evidence to indicate a difference in the two flexural strength distributions. No obvious change in the flexural strength seemingly results from the offset between the strengthening mechanism and the weakening mechanism. In monolithic SiC specimens, some researchers [21–23] reported that the surface oxidation could either increase or decrease the flexural strength. The final results are affected by the partial pressure of oxygen, exposure time, and specimen composition. In the present work, the phenomenon of the flexural strength increase was not observed. Thus, further study is needed on the oxidation-induced strength change of SiC whisker/Al_2O_3 composites.

5. Conclusions

The effects of surface oxidation on the mechanical properties of SiC whisker/Al_2O_3 composites have been studied.

1. SiC whisker–oxygen–alumina reaction produces a surface layer on tested composite specimens. The layer reveals the presence of oxidation-induced bubbles and is in a state of compressive residual stress.

2. Thermal quenching into a water bath shows that the specimens oxidized at 1450 °C for 85 h have better thermal shock resistance than the non-oxidized specimens. The improvement is due to the fact that the surface oxidation layer significantly decreases the surface heat-transfer coefficient.

3. The specimens with oxidation treatment at 1450 °C for 85 h exhibit a strength degradation, as compared with the as-polished specimens. The oxidation-induced bubbles mainly account for the weakening mechanism. However, statistical analysis indicates that there is insufficient evidence to indicate a strength degradation occurring in the specimens oxidized at 1450 °C for 2 h. This is attributed to the fact that the strengthening mechanism, induced from surface-crack healing and surface compressive residual stress, offsets the weakening mechanism.

Acknowledgements

The author thanks Andre Ezis, Cercom Incorporated, Vista, CA, for providing SiC whisker/Al_2O_3 composites, and Frank Fandetti, Hoechst CeramTec North America Incorporated, Mansfield, MA, for providing alumina substrates.

References

1. P. F. BECHER, C. H. HSUEH, P. ANGELINI and T. N. TIEGS, *J. Am. Ceram. Soc.* **71** (1988) 1050.
2. G. H. CAMPBELL, M. RUHLE, B. J. DALGLEISH and A. G. EVANS, *ibid.* **73** (1990) 521.
3. M. T. SYKES, R. O. SCATTERGOOD and J. L. ROUTBORT, *Composites* **18** (1987) 153.
4. R. K. GOVILA, *J. Mater. Sci.* **23** (1988) 3782.
5. P. F. BECHER, P. ANGELINI, W. H. WARWICK and T. N. TIEGS, *J. Am. Ceram. Soc.* **73** (1990) 91.
6. K. JAHUS and S. V. NAIL, *Compos. Sci. Technol.* **37** (1990) 279.
7. T. TIEGS and P. F. BECHER, *J. Am. Ceram. Soc.* **70** (1987) C109.
8. C. C. CHIU and C. S. CHIU, *J. Compos. Mater.*, in press.
9. D. LEWIS, *Am. Ceram. Soc. Bull.* **58** (1979) 599.
10. C. C. CHIU, *J. Am. Ceram. Soc.* **73** (1990) 1999.
11. *Idem, J. Mater. Sci.* **28** (1993) 5684.
12. W. J. LEE and E. D. CASE, *ibid.* **25** (1990) 5043.
13. K. MATSUSHITA, S. KURATANI, T. OKAMOTO and M. SHIMADA, *J. Mater. Sci. Lett.* **3** (1984) 345.
14. C. C. CHIU and E. D. CASE, *J. Mater. Sci.* **27** (1992) 2353.
15. "Standard Test Method for Young's Modulus, Shear Modulus, and Poisson's Ratio for Glass and Glass-Ceramic by Resonance", Annual Book of ASTM Standard, Designation: C623-71, reapproved 1981. (American Society for Testing and Materials, Philadelphia, PA, 1981).
16. W. HWANG and K. S. HAN, *Composites* **18** (1987) 47.
17. R. D. DOREMUS, *J. Appl. Phys.* **54** (1983) 193.
18. H. . NEAVE and P. L. WORTHINGTON, "Distribution-Free Tests" (Unwin Hyman, Winchester, MA, 1988) pp. 109–13.
19. D. HAN and J. J. MECHOLSKY, *J. Am. Ceram. Soc.* **73** (1990) 3692.
20. M. M. TOJEK and D. J. GREEN, *ibid.* **72** (1989) 1885.
21. R. FORTHMANN and A. NAOUMIDIS, *Mater. Sci. Eng.* **A121** (1989) 457.
22. T. E. EASLER, R. C. BRADT and R. E. TRESSLER, *J. Am. Ceram. Soc.* **64** (1981) 731.
23. H. E. KIM and A. J. MOORHEAD, *ibid.* **73** (1990) 1868.

Received 7 October 1992
and accepted 19 October 1993